



HAL
open science

Megafloods in Europe can be anticipated from observations in hydrologically similar catchments

Miriam Bertola, Günter Blöschl, Milon Bohac, Marco Borga, Attilio Castellarin, Giovanni B Chirico, Pierluigi Claps, Eleonora Dallan, Irina Danilovich, Daniele Ganora, et al.

► To cite this version:

Miriam Bertola, Günter Blöschl, Milon Bohac, Marco Borga, Attilio Castellarin, et al.. Megafloods in Europe can be anticipated from observations in hydrologically similar catchments. *Nature Geoscience*, 2023, 16, pp.982-988. 10.1038/s41561-023-01300-5 . hal-04344730

HAL Id: hal-04344730

<https://hal.inrae.fr/hal-04344730>

Submitted on 14 Dec 2023

HAL is a multi-disciplinary open access archive for the deposit and dissemination of scientific research documents, whether they are published or not. The documents may come from teaching and research institutions in France or abroad, or from public or private research centers.

L'archive ouverte pluridisciplinaire **HAL**, est destinée au dépôt et à la diffusion de documents scientifiques de niveau recherche, publiés ou non, émanant des établissements d'enseignement et de recherche français ou étrangers, des laboratoires publics ou privés.

Megafloods in Europe can be anticipated from observations in hydrologically similar catchments

Author list

Miriam Bertola^{1*}, Günter Blöschl¹, Milon Bohac², Marco Borga³, Attilio Castellarin⁴, Giovanni B. Chirico⁵, Pierluigi Claps⁶, Eleonora Dallan³, Irina Danilovich⁷, Daniele Ganora⁶, Liudmyla Gorbachova⁸, Ondrej Ledvinka^{2,9}, Maria Mavrova-Guirguinova¹⁰, Alberto Montanari⁴, Valeriya Ovcharuk¹¹, Alberto Viglione⁶, Elena Volpi¹², Berit Arheimer¹³, Giuseppe Tito Aronica¹⁴, Ognjen Bonacci¹⁵, Ivan Čanjevac¹⁶, Andras Csik¹⁷, Natalia Frolova¹⁸, Boglarka Gmandt¹⁷, Zoltan Gribovszki¹⁹, Ali Gül²⁰, Knut Günther²¹, Björn Guse^{21,22}, Jamie Hannaford^{23,24}, Shaun Harrigan²⁵, Maria Kireeva¹⁸, Silvia Kohnová²⁶, Jürgen Komma¹, Jurate Kriauciuniene²⁷, Brian Kronvang²⁸, Deborah Lawrence²⁹, Stefan Lüdtke²¹, Luis Mediero³⁰, Bruno Merz^{21,31}, Peter Molnar³², Conor Murphy²⁴, Dijana Oskoruš^{33,34}, Marzena Osuch³⁵, Juraj Parajka¹, Laurent Pfister³⁶, Ivan Radevski³⁷, Eric Sauquet³⁸, Kai Schröter³⁹, Mojca Šraj⁴⁰, Jan Szolgay²⁶, Stephen Turner²³, Peter Valent¹, Noora Veijalainen⁴¹, Philip J. Ward^{42,43}, Patrick Willems⁴⁴, Nenad Zivkovic⁴⁵.

Affiliations

¹Institute of Hydraulic Engineering and Water Resources Management, Technische Universität Wien, Vienna, Austria.

²Czech Hydrometeorological Institute, Prague, Czechia.

³Department of Land, Environment, Agriculture and Forestry, University of Padova, Padua, Italy

⁴Department of Civil, Chemical, Environmental and Materials Engineering (DICAM), Università di Bologna, Bologna, Italy.

⁵Department of Agricultural Sciences, University of Naples Federico II, Naples, Italy.

⁶Department of Environment, Land and Infrastructure Engineering (DIATI), Politecnico di Torino, Turin, Italy.

⁷Climate Research Laboratory, Institute for Nature Management, The National Academy of Science of Belarus, Minsk, Belarus.

⁸Department of Hydrological Research, Ukrainian Hydrometeorological Institute, Kyiv, Ukraine.

⁹Department of Physical Geography and Geoecology, Faculty of Science, Charles University, Prague, Czechia.

¹⁰University of Architecture, Civil Engineering and Geodesy, Sofia, Bulgaria.

¹¹Hydrometeorological Institute, Odessa State Environmental University, Odessa, Ukraine.

¹²Department of Engineering, University Roma Tre, Rome, Italy.

¹³Swedish Meteorological and Hydrological Institute, Norrköping, Sweden.

¹⁴Department of Engineering, University of Messina, Messina, Italy.

¹⁵Faculty of Civil Engineering, Architecture and Geodesy, Split University, Split, Croatia.

¹⁶Department of Geography, Faculty of Science, University of Zagreb, Zagreb, Croatia.

¹⁷General Directorate of Water Management, Budapest, Hungary.

¹⁸Department of Land Hydrology, Lomonosov Moscow State University, Moscow, Russia.

- 43 ¹⁹University of Sopron, Faculty of Forestry, Institute of Geomatics and Civil Engineering, Sopron, Hungary.
- 44 ²⁰Department of Civil Engineering, Faculty of Engineering, Dokuz Eylul University, Izmir, Turkey.
- 45 ²¹Helmholtz Centre Potsdam, GFZ German Research Centre for Geosciences, Section Hydrology, Potsdam,
- 46 Germany.
- 47 ²²Department of Hydrology and Water Resources Management, Institute for Natural Resource Conservation, Kiel
- 48 University, Kiel, Germany
- 49 ²³Centre for Ecology and Hydrology, Wallingford, UK.
- 50 ²⁴Irish Climate Analysis and Research Units (ICARUS), Department of Geography, Maynooth University,
- 51 Maynooth, Ireland.
- 52 ²⁵Forecast Department, European Centre for Medium-Range Weather Forecasts (ECMWF), Reading, UK.
- 53 ²⁶Department of Land and Water Resources Management, Faculty of Civil Engineering, Slovak University of
- 54 Technology in Bratislava, Bratislava, Slovakia.
- 55 ²⁷Lithuanian Energy Institute, Kaunas, Lithuania
- 56 ²⁸Department of Ecoscience, Danish Centre for Environment and Energy, Aarhus University, Aarhus, Denmark.
- 57 ²⁹Norwegian Water Resources and Energy Directorate, Oslo, Norway.
- 58 ³⁰Department of Civil Engineering: Hydraulic, Energy and Environment, Universidad Politécnica de Madrid,
- 59 Madrid, Spain.
- 60 ³¹Institute of Environmental Sciences and Geography, University Potsdam, Potsdam, Germany
- 61 ³²Institute of Environmental Engineering, ETH Zurich, Zurich, Switzerland.
- 62 ³³Department of Hydrotechnics, Faculty of Geotechnical Engineering, University of Zagreb, Varaždin, Croatia.
- 63 ³⁴Croatian Meteorological and Hydrological Service, Zagreb, Croatia.
- 64 ³⁵Department of Hydrology and Hydrodynamics, Institute of Geophysics Polish Academy of Sciences, Warsaw,
- 65 Poland.
- 66 ³⁶Luxembourg Institute of Science and Technology (LIST), Esch-sur-Alzette, Luxembourg.
- 67 ³⁷Institute of Geography, Faculty of Natural Sciences and Mathematics, Ss. Cyril and Methodius University,
- 68 Skopje, North Macedonia.
- 69 ³⁸Irstea, UR RiverLy, Lyon-Villeurbanne, France.
- 70 ³⁹Leichtweiss Institute for Hydraulic Engineering and Water Resources, Technische Universität Braunschweig,
- 71 Braunschweig, Germany.
- 72 ⁴⁰Faculty of Civil and Geodetic Engineering, University of Ljubljana, Ljubljana, Slovenia.
- 73 ⁴¹Finnish Environment Institute, Helsinki, Finland.
- 74 ⁴²Institute for Environmental Studies (IVM), Vrije Universiteit Amsterdam, The Netherlands.
- 75 ⁴³Deltares, Delft, The Netherlands.
- 76 ⁴⁴Department of Civil Engineering, KU Leuven, Leuven, Belgium.
- 77 ⁴⁵Faculty of Geography, University of Belgrade, Belgrade, Serbia.
- 78 *Corresponding author. E-mail: bertola@hydro.tuwien.ac.at

79
80

81 **Abstract**

82 Mega-floods that far exceed previously observed records often take citizens and
83 experts by surprise, resulting in extremely severe damage and loss of life. Existing
84 methods based on local and regional information rarely go beyond national borders
85 and cannot predict these floods well because of limited data on mega-floods, and
86 because flood generation processes of extremes differ from those of smaller, more
87 frequently observed events. Here we analyse river discharge observations from over
88 8000 gauging stations across Europe and show that recent mega-floods could have
89 been anticipated from those previously observed in other places of Europe. Almost all
90 observed mega-floods (95.5%) fall within the envelope values estimated from previous
91 floods at other similar places on the continent, implying that local surprises are not
92 surprising at the continental scale. This holds also for older events, indicating that
93 mega-floods have not changed much in time relative to their spatial variability. The
94 underlying concept of the study is that catchments with similar flood generation
95 processes produce similar outliers. It is thus essential to transcend national
96 boundaries and learn from other places across the continent to avoid surprises and
97 save lives.

98

99 **Main Text**

100 Mega-floods that are much larger than floods experienced previously in a given
101 catchment or region, can take citizens and local flood managers by surprise, resulting
102 in catastrophic damage and loss of life. For example, the discharge of the July 2021
103 flood at the Rhine tributaries in Germany, and rivers in the Netherlands, Belgium and
104 Luxembourg, was up to four times larger than any event on record in the region¹,
105 causing almost 200 fatalities and damage in excess of \$40 billion. In this and other
106 cases, the lack of previous local experience of events of this magnitude resulted in
107 insufficient flood defence measures, preparedness and real-time response^{1,2}.

108 Because of their rare occurrence, mega-floods are difficult to predict. The standard
109 method of estimating the magnitude of potential large floods consists of fitting a
110 probability distribution to long series of flood observations, and extrapolating the
111 distribution to small probabilities³. However, long series that include several
112 exceptional events are rarely available. Some estimation methods use flood
113 observations from neighbouring catchments⁴, to make up for the brevity of streamflow
114 records which, however, rarely increases the chances of capturing mega-floods. Even
115 when such events are observed, accurate discharge estimates are difficult to obtain
116 as the flood wave may partially bypass the gauge and difficulties with extrapolating the
117 rating curve. Moreover, the processes that generate extreme floods tend to differ from
118 those that generate smaller and more frequent events⁵, making extrapolation
119 notoriously inaccurate. One way of capturing changing flood processes with
120 magnitude is through rainfall-runoff models, but they require long series of precipitation
121 and are also subject to uncertainty^{6,7,8}. Large floods in historic or prehistoric times

122 (paleofloods) can also be used, although the information available is often not
123 commensurate with the requirements of flood management^{9,10,11}.

124 An alternative for enhancing the accuracy of megaflood estimates is the transfer of
125 flood information from hydrologically similar catchments where large events may have
126 occurred⁴. In Europe the occurrence of megafloods is well documented at the national
127 scale. The August 2002 flood in Germany, Austria and Bohemia was the largest in the
128 last half century based on economic losses; the November 1994 Piedmont flood was
129 the second costliest event in Europe between 1970 and 2020¹². Both events were
130 caused by rainfall greater than one-third of the annual total, delivered in only 72
131 hours^{13,14}. However, flood information transfer rarely goes beyond national borders,
132 and no previous study has examined megafloods in a systematic way across an entire
133 continent, with the objective of learning from other places about the potential of future
134 flood surprises. Some examples comparing the world's maximum measured floods
135 also exist¹⁵, but they do not compare hydrologically similar catchments, which makes
136 flood estimation less useful for practical purposes.

137

138 **Anticipating megafloods**

139 Here we analyse the most comprehensive dataset of annual maximum discharges in
140 Europe available to date and show that recent megafloods could have been
141 anticipated from observations in other parts of Europe, which would not be possible
142 using national data only. We also show that the predictability of megafloods does not
143 change in time when sub-periods are analysed. We base our analysis on annual
144 maximum river discharge observations from 8023 gauging stations for the period
145 1810–2021. The average length of the series is 51.4 years and the catchment areas
146 range between 1 km² and 800,000 km². Catchments across Europe are grouped into
147 five hydroclimatic regions (Fig. 1) as a first step of identifying hydrologically similar
148 catchments¹⁶. For each region, we estimate a regional envelope curve of flood
149 discharges that represents the relationship between flood discharge and catchment
150 area that is not exceeded by any observed flood in the region (see Methods; Extended
151 Data Table 2). To examine possible changes in time, we also compare envelope
152 curves obtained using observations from two 30-year sub-periods, i.e., 1961-1990 and
153 1991-2020.

154 We focus on 498 catchments (“target” catchments) where 510 recent (i.e. after 1999)
155 megafloods that are surprising based on local data are identified (see Methods). To
156 evaluate the possibility of anticipating megafloods in target catchments using
157 information from other places in Europe, we perform a hindcast experiment of
158 predicting their peak discharge with regional envelope curves, using flood
159 observations from similar catchments up to the year before their occurrence. For each
160 target catchment, a group of similar catchments (“donor” catchments) is identified in
161 the corresponding hydroclimatic region based on the similarity of catchment area and
162 the mean and coefficient of variation of the truncated flood series (up to the year before
163 the megaflood). From this group of donor catchments we construct an envelope curve

164 which we compare with the megaflood that occurred later in the target catchments.
165 We repeat this analysis for all 510 detected megafloods in the target catchments.

166

167 **European envelope curves of flood discharges**

168 Our data show that recent megafloods have occurred in all regions of Europe, although
169 they are more frequent in the Atlantic and Continental regions (Fig.1; Extended Data
170 Table 3), where respectively 8.7% and 7.2% of the catchments exhibit recent
171 megafloods. In the Boreal region, the respective value is only 1.3%. The smaller value
172 is related to the smaller interannual variability of floods in the Boreal region¹⁷.

173 In the Atlantic region, the megafloods (coloured points in Fig. 1b-f) are on average 3.4
174 times larger than the local mean annual maximum discharges (squares), while in the
175 Continental and Mediterranean regions they are 5.3 and 5.2 times larger (Extended
176 Data Table 3). The larger ratio in the Mediterranean is likely related to the more non-
177 linear rainfall-runoff process and more variable precipitation in arid than in humid
178 climates^{5,18}. However this analysis is not able to conclude whether megafloods are
179 becoming more frequent or not.

180 The envelope curves defined by the largest floods also differ between hydroclimatic
181 regions in terms of their intercept and slope (thick continuous lines in Fig. 1b-f;
182 Extended Data Table 2). For a catchment size of 1000 km², the envelope specific
183 discharge in the Mediterranean region is 5.26 m³s⁻¹km⁻² while in the Boreal region it is
184 1.37 m³s⁻¹km⁻². This is because the flood-inducing rainstorms in the Mediterranean
185 are associated with much larger intensities than the flood-inducing snowmelt typical of
186 Northern Europe. The slopes of the envelope curves are steepest in the Mediterranean
187 area (-0.57) and flattest (-0.07) in the Boreal region (Fig. 1). This is because the
188 Mediterranean rainstorms tend to be more localised than the snowmelt in the North of
189 Europe. The envelope curves for the most recent sub-period (thin dotted lines) tend to
190 be slightly lower than those for the first sub-period (thin dashed lines), except for the
191 Mediterranean and the Atlantic region. The median regression curves (thin continuous
192 lines) are slightly flatter than the respective envelopes, as larger catchments tend to
193 have more regular flood regimes than small ones. Figs. 1g-j illustrate examples of flood
194 series in pairs of catchments with and without megafloods.

195 To illustrate the potential of anticipating megafloods from other places in Europe, Fig.
196 2 shows three examples. The 2002 flood in the Kamp catchment in Austria (Fig. 2a)
197 peaked at 459 m³s⁻¹ which is equivalent to a specific discharge of 0.74 m³s⁻¹km⁻² (black
198 triangle) given the catchment area of 622 km². The envelope curve (blue line), defined
199 by the hydrologically similar catchments within the hydroclimatic region, gives a
200 specific discharge of 1.68 m³s⁻¹km⁻². This means that, in light of European floods, the
201 Kamp was not at all surprising while for the locals it was¹⁹. The regional envelope
202 discharge illustrated in Fig. 2 is defined based on previously observed floods in various
203 European countries, including Bulgaria and Poland (blue circles in Fig. 2d).

204 The 2009 flood in the Cumbrian Derwent catchment in the UK (Fig. 2b) peaked at 0.84
205 $\text{m}^3\text{s}^{-1}\text{km}^{-2}$ and was 58% larger than the second largest event on record which occurred
206 in 2005. The corresponding envelope specific discharge is $1.64 \text{ m}^3\text{s}^{-1}\text{km}^{-2}$. Much larger
207 extremes were observed in similar catchments in Norway (Fig. 2e). The 2009
208 megaflood in the Derwent was itself exceeded in 2015, however this later event still
209 lies below the envelope curve and was not as surprising as the 2009 event (11%
210 larger)².

211 The 2021 flood in the Ahr catchment in Germany (Fig. 2c) peaked at $0.80 \text{ m}^3\text{s}^{-1}\text{km}^{-2}$,
212 similar to the Kamp flood, with an envelope estimate of $1.57 \text{ m}^3\text{s}^{-1}\text{km}^{-2}$. For the Ahr
213 catchment, the similar catchments making up the donor group are, in descending order
214 of flood magnitude: the Timis in Romania, the Freiburger Mulde in Germany, the
215 Maritsa in Bulgaria, the Ljig in Serbia, the Lausitzer Neisse in Germany, the Corrèze
216 and Le Lot in France, the Nysa Kłodzka in Poland and the Birs in Switzerland (Fig. 3).
217 Although each of these catchments has a specific hydrological behaviour, overall they
218 can be considered hydrologically similar to the Ahr in terms of average climate and
219 flood statistical properties. All of these ten catchments experienced record-breaking
220 floods that were surprising based on previously observed events at that location, and
221 these occurred in the period before 2021 (Fig. 3).

222 The analysis of Fig. 2 is repeated for all 510 recent megafloods in the target
223 catchments in Europe (Fig. 4). In 95.5% of the target catchments, the discharge of the
224 envelope is larger than that of the observed megaflood, suggesting that, from a
225 European perspective, almost none of the events can be considered a regional
226 surprise. In 9.6% of the cases, the observed megafloods are within 75% and 150% of
227 the envelope (red points in Fig. 4a), i.e. the order of magnitude is similar. The target
228 catchments are distributed all over Europe with a higher concentration in the West
229 (Fig. 4b), reflecting positive trends in flood magnitudes in Western Europe^{20,21} and, to
230 some degree, the higher station density.

231 The prediction is also conducted for 151 and 188 catchments with 151 and 190 recent
232 (i.e. in the last 10 years of each sub-period) megafloods in the first and second sub-
233 period, respectively. The distribution of the ratio between observed and predicted
234 discharge (inset of Fig. 4a) indicates that there are no substantial changes in the
235 predictability of megafloods in time. The discharge of the envelope is larger than that
236 of the observed megaflood in 92% and 93.7% of the respective target catchments.

237 To evaluate the suitability of the donor selection, we compare the timing within the
238 year of the target megafloods with that of the ten largest floods in the donor catchments
239 (Fig. 4c). Flood timing is a proxy of flood generation processes²². Fig. 4c shows that
240 the timing of the target megafloods (black lines) generally agrees with that of the
241 donors (brown lines), both in terms of the average timing (angle from the centre of the
242 circle) and the consistency of timing between events (distance to the centre). The
243 agreement points towards the plausibility of the donor selection and prediction. A
244 tendency for the observed timings to be more bimodal than the predictions is likely
245 related to the smaller number of events.

246

247 **Implications of expanding the perspective**

248 Whereas previous studies have assessed the potential for megafloods mainly based
249 on local or regional data, this study expands the observation area to the continental
250 scale. We use megafloods that have occurred in hydrologically similar catchments
251 elsewhere on the continent as a surrogate for the megafloods that could happen in the
252 catchment of interest in the future.

253 The degree to which this transfer of information is possible depends on the suitable
254 choice of donor catchments based on the notion of hydrological similarity²³. The
255 underlying concept is that catchments with similar flood generation processes,
256 including rainfall, infiltration and flow paths, produce similar outliers, as these
257 processes determine the transition from smaller to larger events^{5,24,25}. Here we use
258 catchment area and the mean and coefficient of variation of the truncated flood series
259 within the same hydroclimatic region as a proxy of similarity in flood generation
260 processes. While other similarity measures exist¹⁶, our donor catchment selection is
261 deemed plausible because of the similarity of the timing within the year of the events,
262 given that timing is a fingerprint of the interplay between climatic and catchment
263 processes²². Additional spot testing of catchment pairs (such as the Ahr catchment in
264 Germany paired with the Timis catchment in Romania) based on prior knowledge from
265 the literature^{1,25} confirms the similarity. To assess robustness of the method we
266 conduct a sensitivity analysis on the parameters of the similarity criteria and the choice
267 of hydroclimatic regions (Extended Data Fig. 1-8). The results show that changing
268 parameters and/or regions may modify individual donor catchments, but the envelope
269 curve that arises from the set of donor catchments is affected much less (see method
270 section for details).

271 The cross-validation experiment conducted here, starting from observed megafloods,
272 withholding them and only using data from floods that have occurred previously,
273 mimics the case of anticipating megafloods that have not yet occurred. We show that
274 it is indeed feasible to estimate the order of magnitude of possible future megafloods.
275 Almost all observed megafloods (95.5%) are smaller than the envelope values
276 estimated, i.e. the local surprises are not surprising at the continental scale. Similar
277 results are found for different sub-periods, indicating that megafloods have not
278 changed much in time relative to their spatial variability within Europe. These findings
279 are in line with recent studies in the US showing little evidence for temporal trends of
280 large floods²⁶.

281 The proposed envelope curve approach complements alternative methods such as
282 regional statistical approaches that spatially interpolate observed discharges⁴ or
283 process-based rainfall-runoff modelling²⁷. These methods provide best estimates of
284 expected floods, while the envelope method reflects a possible worst case – which
285 itself is an important aspect of flood risk planning.

286 The focus on a possible worst case implies that the envelope values are generally too
287 large to serve as design values for most types of flood defence infrastructure from a
288 cost-benefit perspective. Rather, they describe a possibility space²⁸ that is prudent to
289 consider as civil protection scenarios, required to organise local preparedness, and
290 for testing the safety of very large dams. They can be used to derive extreme flood
291 hazard scenarios, either failure scenarios (what can go wrong?) or future development
292 scenarios (what could the future look like?) that could strengthen existing methods
293 such as the Probable Maximum Flood (PMF) concept²⁹. There is an increasing need
294 for considering the extremes of the extremes, as there is a tendency in society for
295 smaller acceptable risks²⁹, so flood risk management should account for the potential
296 of surprises and their devastating consequences. This requires a shift in thinking²⁹ and
297 the application of envelope curves, storylines^{2,30} and compound event analyses³¹.
298 Making individuals and societies more robust against surprises therefore goes beyond
299 the design of spillways and flood management plans.

300 In summary, to anticipate megafloods we must learn from other places in order to
301 reduce the surprise factor of their occurrence, increase flood risk awareness and
302 enhance preparedness of flood risk management. To this end, it is essential to move
303 beyond national flood risk assessment and share information on megafloods across
304 countries and continents.

305

306 **Acknowledgements**

307 We acknowledge all flood data providers listed in Extended Data Table 1. G. Blöschl and M. Bertola
308 were supported by the FWF projects 'SPATE' (I 3174, I 4776) and W1219-N22. B. Merz and B.
309 Guse were supported by the DFG 'SPATE' project (FOR 2416). A. Viglione, P. Claps, D. Ganora,
310 M. Borga and E. Dallan were supported by the European Union Next-GenerationEU 'RETURN'
311 Extended Partnership (National Recovery and Resilience Plan – NRRP, Mission 4, Component
312 2, Investment 1.3 – D.D. 1243 2/8/2022, PE0000005). S. Kohnová and J. Szolgay were supported
313 by the Slovak Research and Development Agency (number APVV-20-0374) and the VEGA Grant
314 Agency (number 1/0782/21). J. Hannaford and S. Turner were supported by the ROBIN (Reference
315 Observatory of Basins for INternational hydrological climate change detection) initiative, with
316 funding from the Natural Environment Research Council (grant number NE/W004038/1). The
317 authors acknowledge the involvement in the data screening process of M. Haas.

318

319 **Author Contributions Statement**

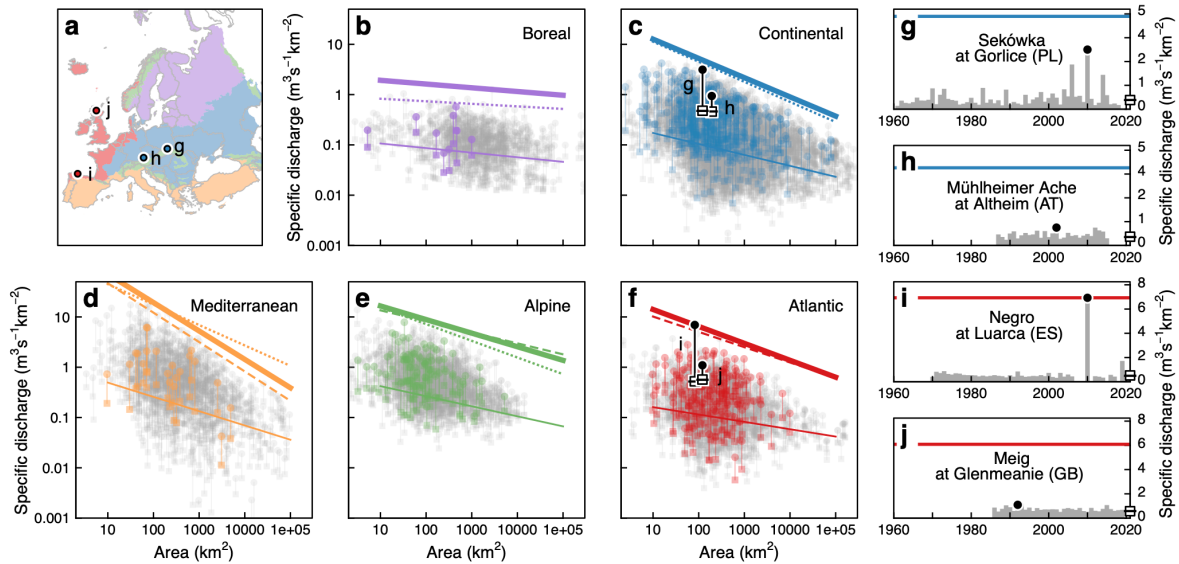
320 G. Blöschl and M. Bertola initiated the study and wrote the first draft of the paper. M. Bertola, G.
321 Blöschl, M. Borga, A.C., P.C., E.D., D.G., A.M., A.V. and E.V. designed the study. M. Bertola
322 collated the updated version of the database with the help of most of the co-authors and conducted
323 the analyses. G. Blöschl, M. Bertola, interpreted the results in the context of underlying geophysical
324 mechanisms. G. Boglarka, M. Boháč, A.C., S.K., O.L., S.L. M.M.-G., K.G., Z.G., B.G., J.K., B.M.,
325 P.M., J.P., L.P., I.R., K.S., J.S., P.V., P. Ward, P. Willems., and N.Ž. interpreted the results in
326 central Europe. G.T.A., O.B., M. Borga, A.C., I.Č., G.B.C., P.C., E.D., D.G., A.G., A.M., L.M., D.O.,
327 M.Š., A.V. and E.V. interpreted the results in southern Europe. B.A., B.K., D.L., and N.V.
328 interpreted the results in northern Europe. J.H., S.H., C.M., S.T., and E.S. interpreted the results
329 in western Europe. I.D., N.F., L.G., M.K., J.K., M.O. and V.O. interpreted the results in eastern
330 Europe. All authors contributed to framing and revising the paper.

331
332

333 Competing Interests Statement

334 The authors declare no competing interests.
335

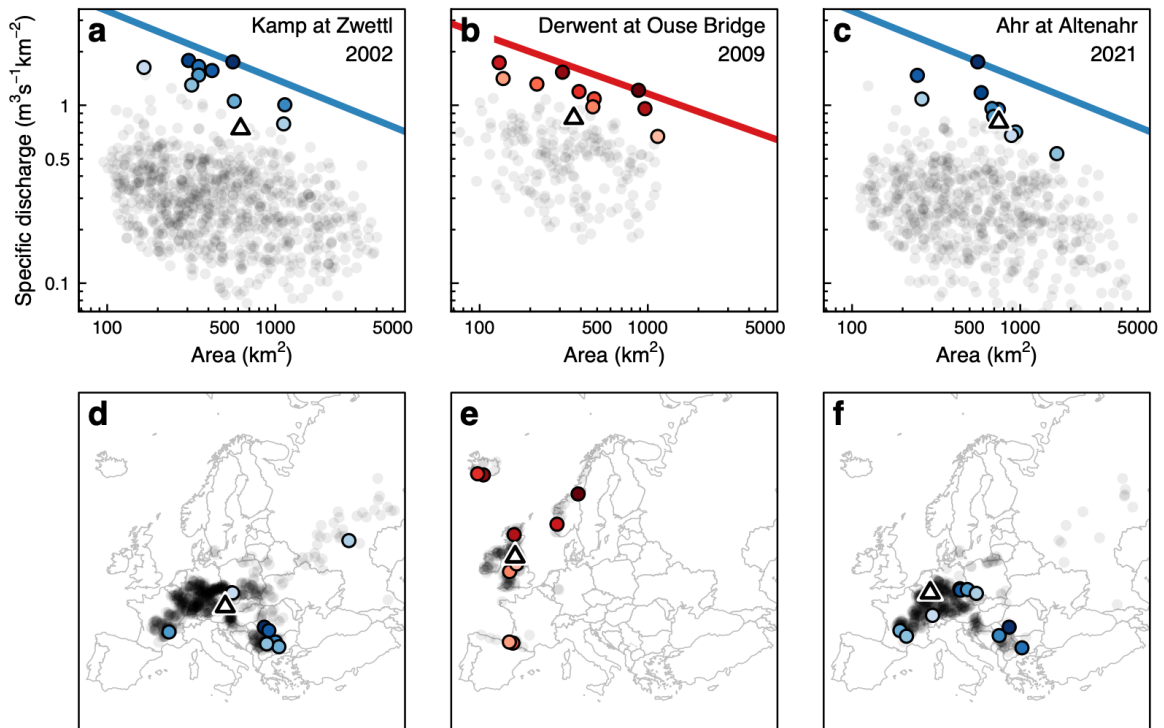
336 Figure Captions



337

338 **Fig. 1: Megafoods in Europe.** (a) Five hydroclimatic regions: Boreal (purple),
339 Continental (blue), Mediterranean (orange), Alpine (green) and Atlantic (red). (b-f)
340 Maximum observed specific flood discharges (points) and mean of annual specific
341 flood discharges (squares) over the entire observation period at each stream gauge
342 as a function of catchment area. Regional envelope curves (thick lines) and median
343 regional annual specific flood discharges (thin lines) for the full record period are
344 shown for each hydroclimatic region. Envelope curves for two 30-year sub-periods are
345 also shown (dashed lines for 1961-1990, dotted lines for 1991-2020). Parameters of
346 the envelope curves are listed in Extended Data Table 2. Coloured symbols indicate
347 the mean and maximum flood discharges in the 498 catchments with recent
348 megafoods, grey points those of the remaining catchments. (g-j) Examples of series
349 of annual flood discharges with (g and i) and without (h and j) megafoods; their
350 corresponding mean (squares) and maximum values (points) are highlighted in black
351 in (c) and (f). The locations of corresponding stream gauges are indicated in (a) by
352 circles.

353



354

355 **Fig. 2: Envelope curves for three catchments with recent megafloods in Europe.**

356 (a,d) Kamp (622 km² catchment area) with 2002 flood; (b,e) Cumbrian Derwent (363

357 km²) with 2009 flood, and (c,f) Ahr (746 km²) with 2021 flood, indicated with triangles.

358 (a-c) Maximum specific discharges observed before the year of occurrence of the

359 megaflood for 824 (a), 196 (b) and 590 (c) similar donor catchments (points) selected

360 within the corresponding hydroclimatic region. Coloured points indicate ten largest

361 events (in terms of distance to the envelope curve), with shades being darker for

362 events that are closer to the envelope.

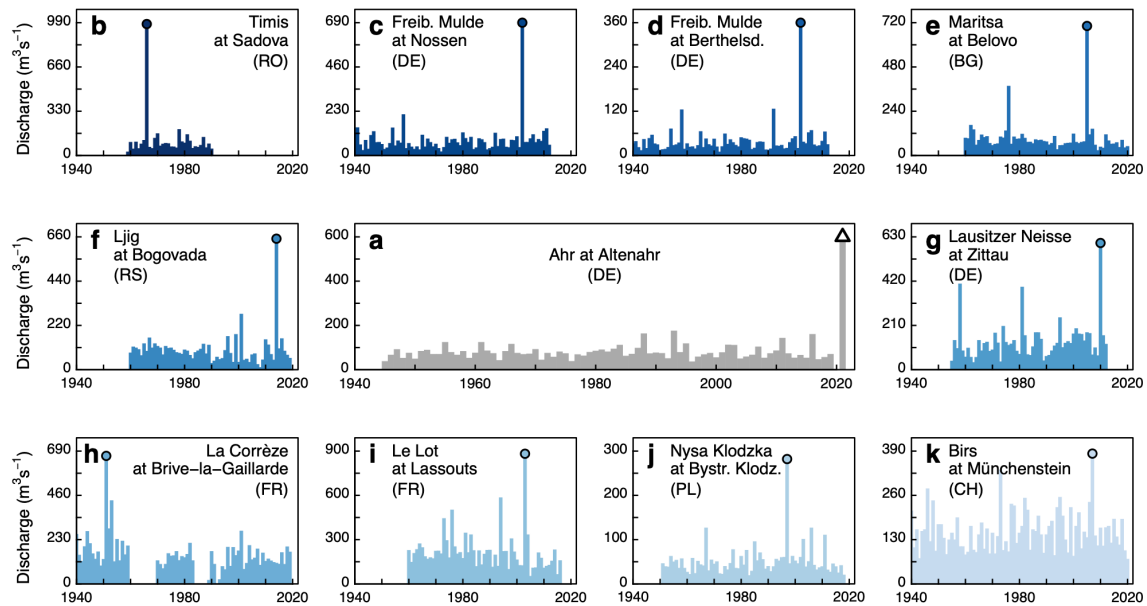
363 Line shows resulting envelope curve with the slope estimated from the hydroclimatic regions (Fig. 1b-f).

364 (d-f) Location of the target (triangle) and donor (points) catchments. Note that the envelope curves of Fig. 1 refer

365 to the entire hydroclimatic region, while here they refer to the donor group within a

366 region.

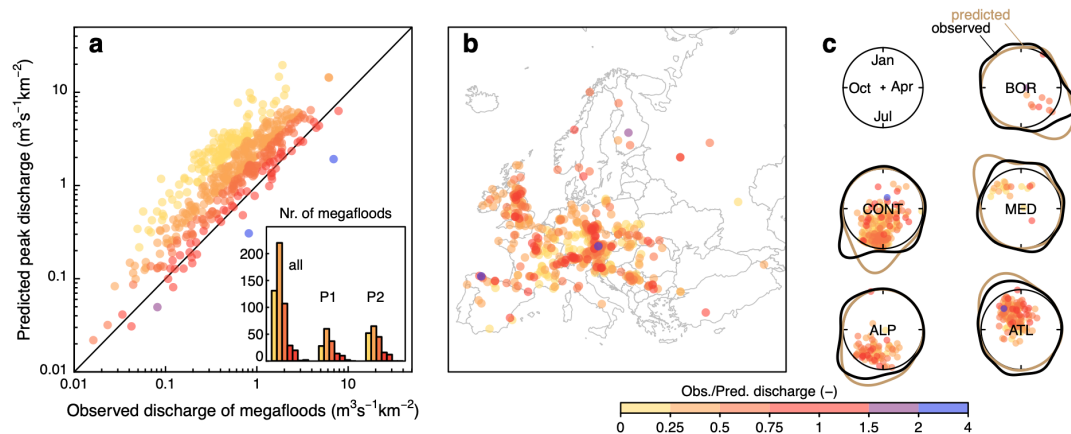
367



368

369 **Fig. 3: Annual flood series for the Ahr and ten donor catchments with extreme**
 370 **floods.** (a) Ahr at Altenahr, Germany, with 2021 mega-flood (the target event) indicated
 371 as a triangle. (b-k) Series for the ten donor catchments indicates as coloured dots in
 372 Fig. 2c,f).

373



374

375 **Fig. 4: Predicted versus observed mega-floods.** (a) Predicted specific envelope
 376 discharge for 498 target catchments versus observed specific discharge of the
 377 mega-floods in the same catchments. Predicted envelope discharges are estimated
 378 using discharge observations from a pool of donor catchments up to the year before
 379 the target mega-flood. The number of target mega-floods is shown in the inset for the
 380 entire period ("all") and the two sub-periods 1961-1990 ("P1") and 1991-2020 ("P2").
 381 Colours indicate the ratio of observed and predicted discharge. (b) Location of target
 382 catchments. Mega-floods occur all over Europe and are less surprising than commonly
 383 assumed. (c) Circular distribution of the timing of the mega-floods observed in the

384 target catchments (black lines), and mean timing of the 10 largest floods in the donor
385 catchments (coloured points) and their distribution (brown lines). The distance of the
386 points to the centre is inversely proportional to the standard deviation of the flood
387 timing.

388
389

390 **References**

- 391 1. Apel, H., Vorogushyn, S., & Merz, B. Brief communication—Impact Forecasting Could
392 Substantially Improve the Emergency Management of Deadly Floods: Case Study July 2021
393 floods in Germany. *Natural Hazards and Earth System Sciences Discussions*, 1-10 (2022).
- 394 2. Kreibich, H., Van Loon, A.F., Schröter, K. et al. The challenge of unprecedented floods and
395 droughts in risk management. *Nature* 608, 80–86 (2022).
- 396 3. De Niel, J., Demarée, G., Willems, P. Weather typing based flood frequency analysis validated for
397 exceptional historical events of past 500 years along the Meuse river, *Water Resources*
398 *Research*, 53(10), 8459-8474 (2017).
- 399 4. Robson, A. J. and Reed, D. W. *Flood Estimation Handbook (FEH)*, chap. Statistical procedures
400 for flood frequency estimation, p. Vol. 3, Institute of Hydrology, Wallingford, UK (1999).
- 401 5. Rogger, M., Pirkl, H., Viglione, A., Komma, J., Kohl, B., Kirnbauer, R., Merz, R., & Blöschl, G.
402 (2012). Step changes in the flood frequency curve: Process controls. *Water Resources Research*,
403 48(5), 1–15.
- 404 6. Bergstrand M., Asp S. and Lindström G. Nationwide hydrological statistics for Sweden with high
405 resolution using the hydrological model S-HYPE. *Hydrology Research*, 45.3, 349-356 (2014).
- 406 7. Devitt, L., Neal, J., Wagener, T., & Coxon, G. Uncertainty in the extreme flood magnitude
407 estimates of large-scale flood hazard models. *Environmental Research Letters*, 16(6), 064013
408 (2021).
- 409 8. Bouaziz, L. et al. Behind the scenes of streamflow model performance, *Hydrol. Earth Syst. Sci.*,
410 25, 1069–1095 (2021).
- 411 9. Kjeldsen, T.R. et al. Documentary evidence of past floods in Europe and their utility in flood
412 frequency estimation. *Journal of Hydrology*, 517, 963–973 (2014).
- 413 10. Blöschl, G., Kiss, A., Viglione et al. Current European flood-rich period exceptional compared with
414 past 500 years. *Nature*, 583(7817), 560–566 (2020).
- 415 11. U.S. Geological Survey Scientific Investigations Report 2020–5065, 89 p. (2020).
- 416 12. World Meteorological Organisation (WMO). *WMO Atlas of Mortality and Economic Losses from*
417 *Weather, Climate and Water Extremes (1970–2019)*. WMO-No. 1267 (2021).
- 418 13. Blöschl, G., Nester, T., Komma, J., Parajka, J., & Perdigão, R. A. P. The June 2013 flood in the
419 Upper Danube Basin, and comparisons with the 2002, 1954 and 1899 floods. *Hydrology and*
420 *Earth System Sciences*, 17(12), 5197–5212 (2013).
- 421 14. Lionetti, M. The Italian floods of 4–6 November 1994. *Weather*, 51(1), 18-27 (1996).
- 422 15. Herschy, R. W. (2002). The world's maximum observed floods. *Flow Measurement and*
423 *Instrumentation*, 13(5–6), 231–235. [https://doi.org/10.1016/S0955-5986\(02\)00054-7](https://doi.org/10.1016/S0955-5986(02)00054-7)
- 424 16. Kuentz, A., Arheimer, B., Hundecha, Y., and Wagener, T. Understanding hydrologic variability
425 across Europe through catchment classification, *Hydrol. Earth Syst. Sci.*, 21, 2863-2879 (2017)

- 426 17. Lun, D., Viglione, A., Bertola, M., Komma, J., Parajka, J., Valent, P., & Blöschl, G. Characteristics
427 and process controls of statistical flood moments in Europe – a data-based analysis. *Hydrology*
428 and *Earth System Sciences*, 25(10), 5535–5560 (2021).
- 429 18. Blöschl, G. Flood generation: process patterns from the raindrop to the ocean, *Hydrol. Earth Syst.*
430 *Sci.*, 26, 2469–2480 (2022)
- 431 19. Blöschl, G. Flood warning - on the value of local information. *International Journal of River Basin*
432 *Management*, 6 (1), pp. 41-50 (2008).
- 433 20. Blöschl, G., Hall, J., Viglione, A. et al. Changing climate both increases and decreases European
434 river floods. *Nature*, 573(7772), 108–111 (2019).
- 435 21. Bertola, M., Viglione, A., Lun, D., Hall, J., & Blöschl, G. Flood trends in Europe: are changes in
436 small and big floods different? *Hydrology and Earth System Sciences*, 24(4), 1805–1822 (2020).
- 437 22. Blöschl, G., Hall, J., Parajka, J., Perdigão, R. A., Merz, B., Arheimer, B., ... & Živkoviæ, N.
438 Changing climate shifts timing of European floods. *Science*, 357(6351), 588-590 (2017).
- 439 23. Blöschl, G., Sivapalan, M., Wagener, T., Viglione, A., Savenije, H.H. *Runoff Prediction in*
440 *Ungauged Basins – Synthesis across Processes, Places and Scales*. Cambridge University Press
441 (2013).
- 442 24. Kemter, M., Merz, B., Marwan, N., Vorogushyn, S., & Blöschl, G. Joint Trends in Flood
443 Magnitudes and Spatial Extents Across Europe. *Geophysical Research Letters*, 47(7), 1–8
444 (2020).
- 445 25. Popescu, I., Jonoski, A., Van Andel, S. J., Onyari, E., & Moya Quiroga, V. G. Integrated modelling
446 for flood risk mitigation in Romania: case study of the Timis–Bega river basin. *International journal*
447 *of river basin management*, 8(3-4), 269-280 (2010).
- 448 26. Collins, M. J., Hodgkins, G. A., Archfield, S. A., & Hirsch, R. M. (2022). The occurrence of large
449 floods in the United States in the modern hydroclimate regime: Seasonality, trends, and large-
450 scale climate associations. *Water Resources Research*, 58,
451 e2021WR030480. <https://doi.org/10.1029/2021WR030480>
- 452 27. Donnelly, C, Andersson, J.C.M. and Arheimer, B. Using flow signatures and catchment similarities
453 to evaluate a multi-basin model (E-HYPE) across Europe. *Hydr. Sciences Journal* 61(2):255-273
454 (2016)
- 455 28. Sivapalan, M., & Blöschl, G. Time scale interactions and the coevolution of humans and water.
456 *Water Resources Research*, 51(9), 6988–7022 (2015).
- 457 29. Merz, B., Vorogushyn, S., Lall, U., Viglione, A., & Blöschl, G. Charting unknown waters-On the
458 role of surprise in flood risk assessment and management. *Water Resources Research*, 51(8),
459 6399–6416 (2015).
- 460 30. Shepherd, T. G. Storyline approach to the construction of regional climate change information.
461 *Proceedings of the Royal Society A*, 475(2225), 20190013 (2019).
- 462 31. Thieken, A. H., Samprogna Mohor, G., Kreibich, H., and Müller, M.: Compound inland flood
463 events: different pathways, different impacts and different coping options, *Nat. Hazards Earth*
464 *Syst. Sci.*, 22, 165–185 (2022).
- 465

466 **Methods**

467

468 **Datasets**

469 The hydrological data used in this study were obtained from a pan-European Flood
470 Database³² with subsequent updates. The current version contains data from 8,023
471 hydrometric gauging stations from 68 European data sources for the period 1810–
472 2021 (Extended Data Table 1). The dataset consists of the highest discharge (daily
473 mean or instantaneous discharge) in each calendar year for each station. The stations
474 are located within the domain bounded by 22.25° W–63.25° E and 34.25° N–71.25° N
475 (Extended Data Fig. 1), and catchment areas range between 1 km² and 800,000 km².
476 The dataset was screened for data errors. The screening involved visual examination
477 of the flood records, analysis of flood seasonality and examination of the gauge
478 location and catchment area in Google Maps. All available stations, including those
479 affected by reservoir construction, were considered for the analysis because reservoir
480 effects were deemed to have little significance for envelope curves for large
481 hydroclimatic regions. Similarly, all available years with data were considered
482 notwithstanding differences in the record lengths, because the focus was on the
483 maxima observations of each series. The minimum series length is 10 years, and the
484 average length is 51.4 years.

485 The gauging stations were grouped into five regions (Fig. 1a; Extended Data Fig.1)
486 that reflect similar hydroclimatic conditions by generalising the European
487 Biogeographical regions³³ with a view on flood processes. The Steppic and Pannonian
488 regions were merged with the Continental region, the Arctic region with the Boreal
489 region, and the Anatolian and Black Sea regions with the Mediterranean region.
490 Additionally, part of northern Italy was considered as part of the Mediterranean region
491 and Iceland as part of the Atlantic region. For comparison, an alternative subdivision
492 of Europe into five regions¹⁷ was considered in a sensitivity analysis (Extended Data
493 Fig. 4a). In order to examine possible changes, the observation period was subdivided
494 into two 30-year sub-periods, P1 (1961-1990) and P2 (1991-2020).

495

496 **Regional envelope curves**

497 We quantified the largest flood events in each region by scaling the peak discharges
498 by catchment area via envelope curves that represent the upper limit of the dataset
499 (Fig. 1):

$$500 \quad \log(q) = a + b \cdot \log(A) \quad (1)$$

501 where q (m³s⁻¹km⁻²) is the specific discharge, i.e. the discharge per unit catchment
502 area A . The parameter b was estimated by quantile regression with quantile $z=0.999$
503 using the `rq` function of the R `quantreg` package^{34,35}. The quantile regression enables
504 a more robust estimate than the tangents on the maxima, because it uses the complete
505 dataset rather than the maxima only. The intercept a was determined such that it

506 satisfies the envelope condition, i.e. the envelope curve is the upper bound of all
 507 observed flood discharges in a region (Extended Data Table 2). For comparison, a
 508 quantile regression with $z=0.5$ is also shown in Fig. 1 (thin line).
 509

510 **Megafloods**

511 For the selection of recent megafloods (Fig. 4) the following criteria were adopted:
 512 (i) the discharge value is a high outlier in the corresponding series of annual maximum
 513 flood discharges, according to the definition³⁶:

$$514 \quad q_{mf} > Q_3 + k * (Q_3 - Q_1) \quad (2)$$

515 where Q_1 and Q_3 are the first and third quartile (i.e. respectively 25% and 75% of the
 516 observations lies below this values) and $k=3$;

517 (ii) the discharge value is record-breaking and locally surprising, i.e., its return period
 518 T_{mf} is at least 3 times larger than the return period of the second largest event up to
 519 that year T_{sl} . The return period was obtained by fitting a GEV distribution to each flood
 520 series up to the year of the megaflood using the L-moments (R extRemes package).

521 (iii) it occurred after the year 1999 (when the full observation period is analysed) and
 522 the corresponding series has at least 20 years of data previous to the event.

523 The selection resulted in a set of 510 megafloods from 498 target catchments, whose
 524 observed specific discharge and location of corresponding gauges are shown in Fig.
 525 4a and 4b. When detecting megafloods in the two 30-year sub-periods, only
 526 observations within each sub-period are considered and the criterion (iii) is modified
 527 such that events in the last 10 years of the respective sub-period are selected (i.e.
 528 after 1979 for P1 and after 2009 for P2).

529 We tested the robustness of the results to the criterion (i) for the selection of high
 530 outliers, using the definition for skewed data³⁷:

$$531 \quad \begin{cases} q_{mf} > Q_3 + 1.5e^{3MC} IQR & \text{if } MC > 0 \\ q_{mf} > Q_3 + 1.5e^{4MC} IQR & \text{if } MC < 0 \end{cases} \quad (3)$$

532 Where MC is the medcouple³⁸, a robust measure of skewness, defined as:

$$533 \quad MC(X_n) = \text{med}_{x_i \leq m_n \leq x_j} h(x_i, x_j) \quad (4)$$

534 with m_n is the sample median of X_n and

$$535 \quad h(x_i, x_j) = \frac{(x_j - m_n) - (m_n - x_i)}{x_j - x_i} \quad (5)$$

536 The alternative selection resulted in a set of 677 megafloods (Supplementary Fig. S1),
 537 whose observed specific discharge and location of corresponding gauges are shown
 538 in Supplementary Fig. S2.

539 We also tested the sensitivity of the results to criterion (ii) for the selection of record-
 540 breaking and surprising events, by varying the threshold T_{mf}/T_{sl} between 1 and 4. The
 541 results of the sensitivity analysis are shown in Supplementary Fig. S3 and indicate
 542 that, when the definition of megafloods is extended to less surprising events (i.e. T_{mf}/T_{sl}
 543 <3), the fraction of megafloods larger than the envelope is unchanged. The only
 544 exception is the Boreal region, where fewer events are selected.

545

546 Donor catchments

547 For each catchment in which a megaflood had occurred (target catchment), a pool of
 548 similar catchments (donor catchments) was identified in the same region. The
 549 similarity between the catchments was quantified in terms of weighted normalised
 550 Euclidean distance D in a three-dimensional space with the following dimensions: the
 551 logarithm of catchment area A , the logarithm of the mean of the annual maximum
 552 specific discharges q_m normalised to a catchment area of 100km², and the coefficient
 553 of variation CV of the annual maximum discharges:

$$554 \quad D = \sqrt{\alpha \left(\frac{\log A_i - \log A_j}{sd(\log A)} \right)^2 + \beta \left(\frac{\log q_{m,i} - \log q_{m,j}}{sd(\log q_m)} \right)^2 + \gamma \left(\frac{CV_i - CV_j}{sd(CV)} \right)^2} \quad (6)$$

555 where i refers to the target catchment, j to a potential donor catchment and sd is the
 556 standard deviation of all catchments in the donor group. Greek letters indicate weights.
 557 q_m and CV were calculated on flood data prior to the year of occurrence of the target
 558 event to obtain a cross-validation experiment that resembles a case of anticipating
 559 megafloods a priori. In estimating q_m and CV we excluded outliers (for both the target
 560 and the donor catchments) according to the criterion of Eq. (2), because megafloods
 561 should not influence the comparison, and only smaller, frequently occurring floods
 562 were used, which is the only information usually available in the case of a prediction.
 563 In selecting the number of catchments in the pooling group, there is a tradeoff between
 564 a larger group that has a higher chance of containing very large floods, and a smaller
 565 group that is hydrologically more homogeneous. For Fig. 1, 2, 3 we used $\alpha=\beta=\gamma=1$
 566 (corresponding to the assumption of the three dimensions having the same
 567 importance) and included catchments with $D < D_{max}$ with $D_{max}=1$, guided by a sensitivity
 568 analysis (see below and Extended Data Fig. 2).

569

570 Megaflood prediction

571 We repeated the selection of the donor group for each target catchment and estimated
 572 the envelope curve, using the slope b of the corresponding hydroclimatic region and
 573 the intercept determined as the minimum that satisfies the envelope condition of the
 574 group only. The procedure only uses observations from donor catchments up to the
 575 year before the megaflood in the target catchment (Fig. 2a-c). We finally obtained an
 576 estimate of the discharge of a potential megaflood in the target catchment (predicted

577 megaflood) from the envelope curve and compared it to the discharge of the observed
578 megaflood (Fig. 4a).

579 In order to evaluate the plausibility of the donor selection we analysed the timing of
580 the megafloods observed in the target and donor catchments using previously
581 established methods²² (Fig. 4c). We compared the distribution of the timing of the
582 observed megafloods to the average timing of the 10 largest floods in the donor group.
583 The circular distributions in Fig. 4c were obtained using the R circular package.

584

585 In order to evaluate the robustness of the method we conducted a number of sensitivity
586 analyses. We varied D_{max} between 0.5 and 1.5 and showed that an increase in D_{max}
587 translates into an increasing number of target megafloods that are below the envelope
588 (Extended Data Fig. 2). The larger fraction in the Boreal region is because of fewer
589 donors available compared to the other regions. We also tested the sensitivity of α , β
590 and γ , examining four weight combinations: equal weights ($\alpha=\beta=\gamma=1$) and doubling
591 one of the weights ($\alpha=2$ and $\beta=\gamma=1$; $\alpha=\gamma=1$ and $\beta=2$; $\alpha=\beta=1$ and $\gamma=2$), which
592 corresponds to the hypothesis of one dimension being more important than the others
593 in the donor selection. There is very little effect on the number of target megafloods
594 below the envelope (Extended Data Fig. 3). While a different set of parameters may
595 modify some of the donor catchments, the resulting envelope curve changes very little.
596 Finally we tested the effect of replacing the regional subdivision of Fig. 1 by an
597 alternative subdivision¹⁷. The analysis shows that the alternative regions may modify
598 the choice of individual donor catchments but, again, the overall conclusions do not
599 change (Extended Data Fig. 4-7).

600

601 **Data availability**

602 The flood discharge data from the data holders/sources listed in Extended Data
603 Table 1 that were used in this paper are available at
604 <https://github.com/tuwhydro/megafloods>.

605

606 **Code availability**

607 The data analysis was performed in R using the supporting packages circular,
608 lubridate, plotrix, quantreg, raster, RColorBrewer, rgdal, rworldmap and scales. The
609 code used can be downloaded from <https://github.com/tuwhydro/megafloods>.

610

611 **Methods-only references**

612 32. Hall, J. et al. A European Flood Database: facilitating comprehensive flood research beyond
613 administrative boundaries. Proc. Int. Assoc. Hydrol. Sci. 370, 89–95 (2015)

- 614 33. Roekaerts, M.: The biogeographical regions map of Europe, in: Basic principles of its creation
615 and overview of its development, European Environment Agency, Copenhagen, available at:
616 [https://www.eea.europa.eu/data-and-maps/ data/biogeographical-regions-europe-3](https://www.eea.europa.eu/data-and-maps/data/biogeographical-regions-europe-3) (2002).
- 617 34. Koenker, R. W. Quantile Regression, Cambridge U. Press (2005).
- 618 35. Amponsah, W., Marra, F., Marchi, L., Roux, H., Braud, I., Borga, M. Objective Analysis of
619 Envelope Curves for Peak Floods of European and Mediterranean Flash Floods. In: Leal
620 Filho, W., Nagy, G., Borga, M., Chávez Muñoz, P., Magnuszewski, A. (eds) Climate Change,
621 Hazards and Adaptation Options. Climate Change Management. Springer, Cham (2020).
- 622 36. Tukey JW. Exploratory Data Analysis. Reading (Addison-Wesley): MA, 1977.
- 623 37. Hubert, M., & Vandervieren, E. (2008). An adjusted boxplot for skewed
624 distributions. Computational statistics & data analysis, 52(12), 5186-5201.
- 625 38. Brys G, Hubert M, Struyf A. A robust measure of skewness. J. Comput. Graph. Stat. 2004;
626 13: 996–1017.